AN APPROACH FOR MONITORING LATERAL SPREADING DUE TO LIQUEFACTION USING STRONG GROUND MOTION RECORDS

Shiro TAKADA[1] And Ryuzo OZAKI[2]

SUMMARY

During earthquakes, lateral spreading due to liquefaction can result in damage to buried pipes or tunnels. Real-time ground motion data can be very helpful for estimating damage for emergency response. In this paper an applied method is proposed for monitoring lateral spreading using a servo velocity seismometer.

In the experimental part of our study, laboratory tests have been done for targeting velocities as 7, 14 and 21 cm/sec (kine). The servo velocity seismometer moves horizontally almost with a constant velocity on a rail with the length of about 2 m to get the records. The primary results showed that the analysis can not simulate the experiment. This is mainly due to the slant of the rail which exerts external pseudo-forces on the pendulum. To take into account the external pseudo-force due to the change of the off-set value, it was measured every 5 cm on the rail. After considering this effect, the analysis results came to good agreement with the test results. The recorded motion during the lateral spreading was different from the actual motion because of the seismometer characteristics, such as a high pass filter. By adding a correction curve for the seismometer characteristics, we were able to match the recorded motion to actual motion.

Therefore, by correcting the characteristics of the servo velocity seismometer, the application of the proposed monitoring method for lateral spreading or permanent ground displacement is proved.

This study serves as the basis for developing real-time warning systems for earthquake deformation of ground.

INTRODUCTION

During earthquakes, lateral spreading due to liquefaction is a cause of damage to buried lifelines such as water and gas mains. Accordingly, the information of ground deformation just after an earthquake will be of great help for estimation of damage and emergency response.

In this study, we sought to develop a prototype system that records movement of the ground. The laboratory tests are conducted to get records when the seismometer is moved horizontally, and the tests are simulated by numerical analysis. Comparing the time history of the single degree of freedom system calculated for the ground motion including the lateral spreading (permanent displacement) with the real time history, the applicability of the method of monitoring for the permanent displacements using the servo velocity seismometer is investigated.

CHARACTERISTICS OF THE SERVO VELOCITY SEISMOMETER

The servo velocity seismometer has a wide dynamic range characteristics and it is able to observe the low frequency (long period) vibration sensitively [Yokoi, 1992]. The circuit of the servo velocity seismometer of

[1] *Department of Architecture & Civil Engineering, Kobe University, Kobe, Japan Email: takada@kobe-u.ac.jp*
[2] *Coastal & Marine Geology, U. S. Geological Survey, Menlo Park, U.S.A Email: rozaki@octopus.wr.usgs.gov*

used in this study is shown in Figure 1, and its parameters used in it are shown in Table 1. C_1 and R_1 are parameters for the differential circuit. R_1, R_3 and R_4 are parameters for the additional circuit. C_2 and R_2 are parameters for integral circuit which is included in the circuit to stabilize the pendulum at the initial position. α is the sensitivity of the gap sensor, and A is the amplification factor of the amplifier. G is the magnetic flux density of the coil. m, k and D are mass of the pendulum, stiffness and damping of the system, respectively [Kagawa, Irikura and Yokoi, 1996].

When the servo velocity seismometer senses the ground motion, the movement of the pendulum is detected by the gap sensor and the output is the voltage which is proportional to the pendulum's movement through the amplifier. A part of output voltage returns to the servo circuit and provide the electric current (which is proportional to the ground acceleration) to the coil in order to attenuate the pendulum movement. Displacement of the pendulum under large attenuation is known to be proportional to the ground velocity. So, above-mentioned output voltage is proportional to the ground velocity [Toki, Sawada, Morikawa and Inukai, 1997].

The mathematical formulation for the seismometer is expressed as follow:

$$\frac{d^2x}{dt^2}+\frac{D}{m}\frac{dx}{dt}+\frac{k}{m}x+\frac{G}{mr}\left(C_1R_4\frac{\alpha Adx}{dt}+\frac{R_4}{R_1}\alpha Ax+\frac{R_4}{C_2R_2R_3}\alpha A\int xdt\right)=-\frac{d^2y}{dt^2} \quad (1)$$

in which x is the displacement of the pendulum and y is the ground displacement. The total sensitivity of the seismometer is shown in Figure 2 while the values of the parameters are in Table 1.

Table 1: Parameters of the seismometer

Parameter	Value	Parameter	Value
R1(ohm)	125000	C2(F)	0.00001
R2(ohm)	20000000	m(kg)	0.03
R3(ohm)	110000	f(Hz)	1.5
R4(ohm)	10000	h	0
r(ohm)	333	G(N/A)	20
C1(F)	0.00001	a A(V/mm)	50

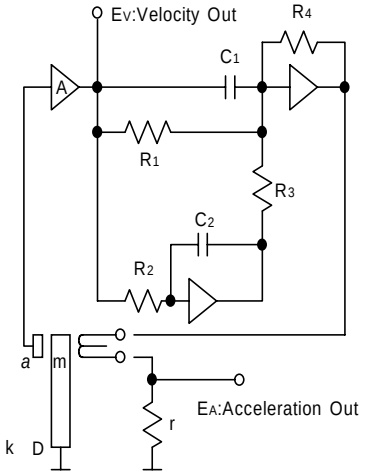

Figure 1: Circuit of the seismometer

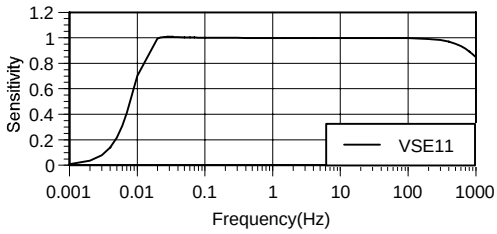

Figure 2: Total sensitivity of the seismometer

LABORATORY TEST AND NUMERICAL ANALYSIS

Laboratory Test of Horizontal Movement of the Servo Velocity Seismometer

In the laboratory test, the servo velocity seismometer is moved horizontally to get records of motions for comparison with a numerical analysis.

Laboratory tests are conducted as shown in the Figure 3. The length of the rail is about 2 m. The wheeled base is settled on the rail and the servo velocity seismometer is put on it. The wheeled base with the servo velocity seismometer is moved horizontally almost with constant speed and the velocity and acceleration are recorded. A displacement meter is located at a fixed point and the actual displacement of seismometer is simultaneously measured.

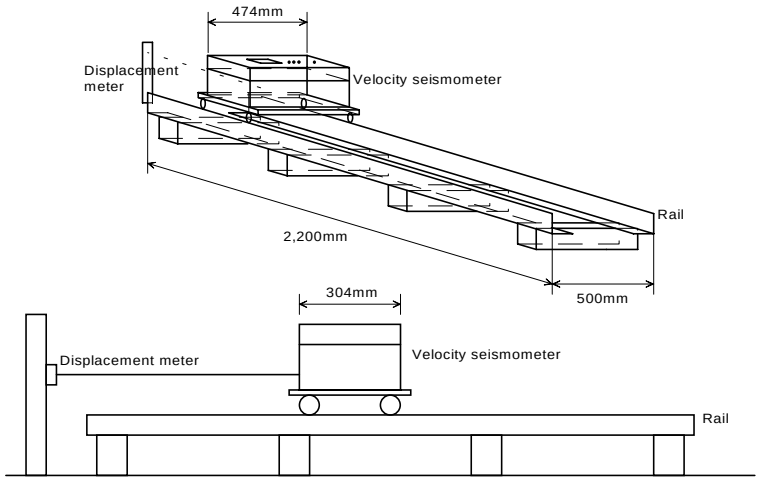

Figure 3: Outline of the laboratory test

The results of three laboratory tests targeting 7, 14 and 21 cm/sec are shown in Figures 4 - 6, respectively. In each of these figures, the recorded velocities by the seismometer and those calculated from the differentiation of displacement meter's records are depicted.

Simulation by Numerical Analysis

Numerical analysis is carried out to simulate the laboratory test. In the numerical analysis using Eq. (1) the external force is equal to that of the laboratory test, using the parameters are used as shown in Table 1. The results are shown in Figures 7 - 9.

Comparing between Figures 7 - 9 with Figures 4 - 6, it is found that the numerical analysis can not simulate the laboratory test. It is considered that the large part of the difference is caused by the very small slant of the rail. The slant of the rail influences the initial position of the pendulum. Whenever it changes, the offset value of the acceleration. So, the slant of the rail gives the external pseudo-forces to the pendulum.

To take into account the external pseudo-force due to the change of offset value, it is measured at every 5 cm on the rail (See Figure 10).

Numerical Analysis taking into account the Change of the Offset Value

The servo velocity seismometer in the author's laboratory has a maximum value of 200 cm/sec for velocity and 2,000 gal for acceleration (10 V for equivalent voltage). When the offset value changes 1 mV, the pseudo-acceleration of 0.2 gal arises. Based on Figure 10, the difference of the offset value between the initial and the final position is about 15 mV. Once the servo velocity seismometer is moved from the initial position to the final position, the pseudo-acceleration of about 3 gal always arises. The results of numerical analysis, taking into account the change of the offset value, are shown in Figures 11 - 13, which present the laboratory test results together. From these figures it is considered that the numerical analysis can simulate the laboratory test

Numerical Analysis taking into account the Change of the Offset Value

The servo velocity seismometer in the author's laboratory has a maximum value of 200 cm/sec for velocity and 2,000 gal for acceleration (10 V for equivalent voltage). When the offset value changes 1 mV, the pseudo-acceleration of 0.2 gal arises. Based on Figure 10, the difference of the offset value between the initial and the final position is about 15 mV. Once the servo velocity seismometer is moved from the initial position to the final position, the pseudo-acceleration of about 3 gal always arises. The results of numerical analysis, taking into account the change of the offset value, are shown in Figures 11 - 13, which present the laboratory test results together. From these figures it is considered that the numerical analysis can simulate the laboratory test.

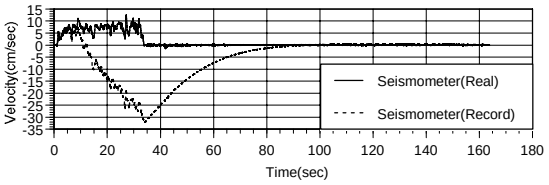

Figure 4: Seismometer record **(No.1, 7cm/sec)**

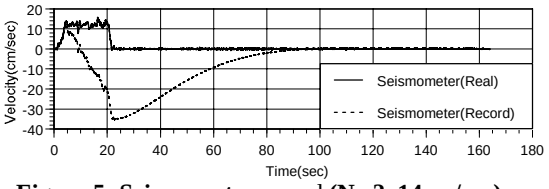

Figure 5: Seismometer record **(No.2, 14cm/sec)**

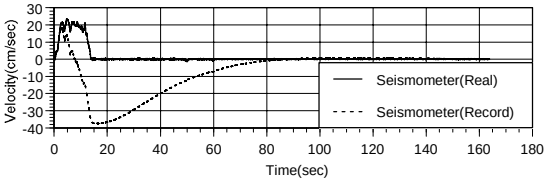

Figure 6: Seismometer record (No.3, 21cm/sec)

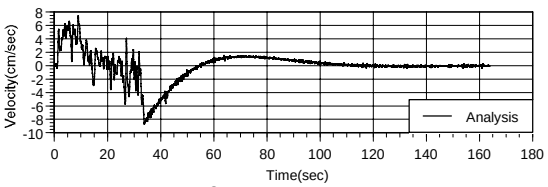

Figure 7: Result of numerical analysis (No.1)

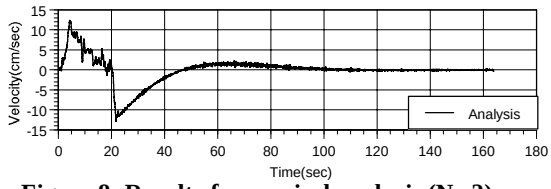

Figure 8: Result of numerical analysis (No.2)

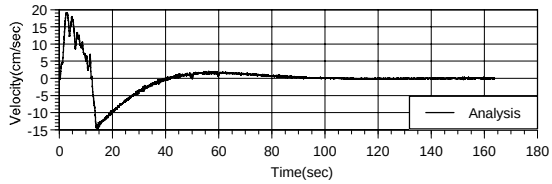

Figure 9: Result of numerical analysis (No.3)

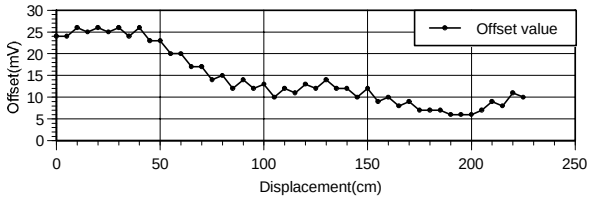

Figure 10: Offset value on the rail

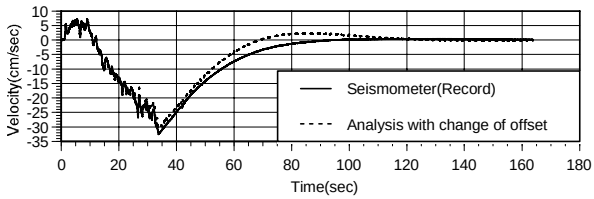

Figure 11: Numerical analysis with offset (No.1)

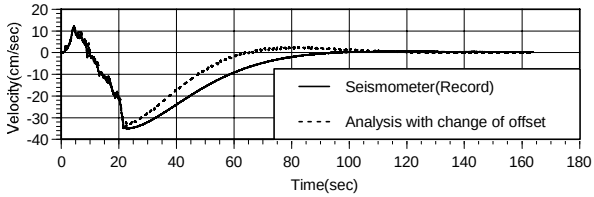

Figure 12: Numerical analysis with offset (No.2)

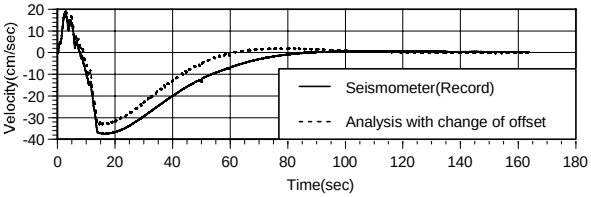

Figure 13: Numerical analysis with offset (No.3)

NUMERICAL ANALYSIS AND SEISMOMETER CORRECTION

Now, because of the lack of the method to grasp the changes of offset value due to the slant of ground lateral spreading, the followings are assumed here. At the time of the lateral spreading, the slant of the ground and the offset change due to it do not occur. And the records can be obtained in the direction of lateral spreading. Based on these assumption, the records at the lateral spreading are simulated by the numerical analysis using Eq. (1) and compared with the input records. Then the measuring method of the permanent ground displacements is investigated.

Movement with a Constant Velocity

First, the case of the movement with a constant velocity is considered. The input and output velocity records are shown in Figure 14(a). The input means the real ground motion and the output is the record of the servo velocity seismometer. In the same way the input and output displacement records are shown in Figure 14(b). From these figures the simulated record does not appear like the actual motion. It is considered that the difference is due to

the seismometer characteristics such as a high pass filter as shown in Figure 1. A curve showing the difference between the real and simulated motion is shown in Figure 14(c).

Some case studies show that the output displacement record (Figure 14(b)) has a similar shape to the correction curve (Figure 14(c), which is given as the difference between input and output velocity records). Figure 14(d) is given by dividing the correction curve by the simulated displacement record. In the case of this displacement record, the curve shown in Figure 14(d) can be closely resembled by a tangent curve. This curve is determined as it closely resembles the infinity at the time that the simulated displacement record crosses zero and is multiplied by the simulated displacement record. So the correction curve can be obtained.

Motion of Laboratory Test

The case that the input motion is given by the laboratory test shown in the preceding part is considered. Results of similar numerical analysis are shown in Figures 15(a) - 17(a). These figures show that the simulated velocity can not express the real one. In the same way by taking into account the correction curve shown in Figures 15(b) - 17(b) the simulated velocity can present the real velocity.

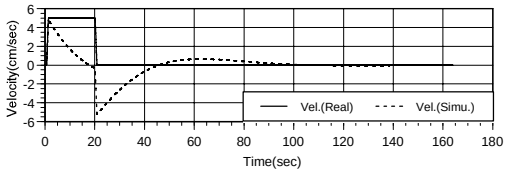

(a) Real and simulated velocity record

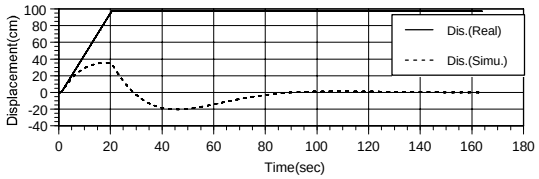

(b) Real and simulated displacement record

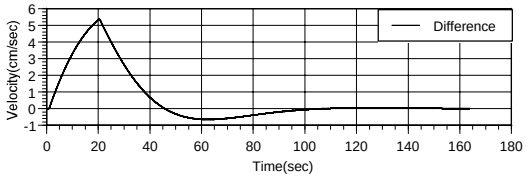

(c) Correction curve

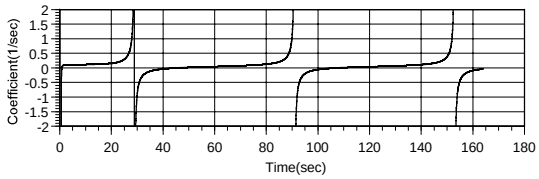

(d) Coefficient curve

Figure 14: Movement with a constant velocity

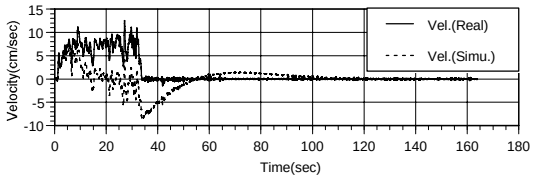

(a) Real and simulated velocity record

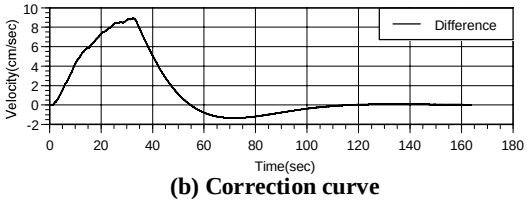

(b) Correction curve

Figure 15: Case of laboratory test (No.1)

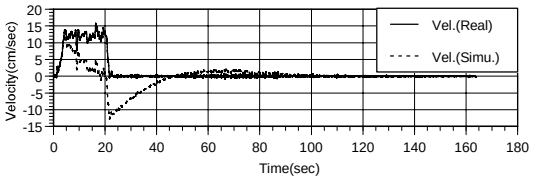

(a) Real and simulated velocity record

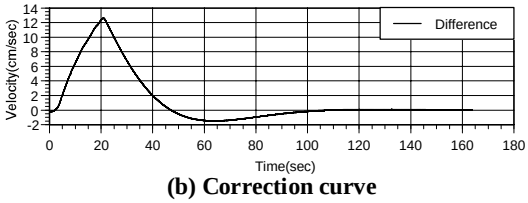

(b) Correction curve

Figure 16: Case of laboratory test (No.2)

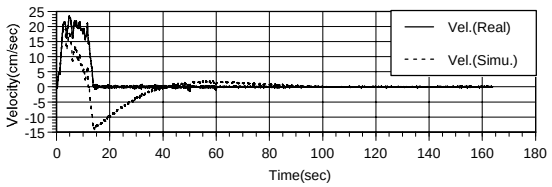

(a) Real and simulated velocity record

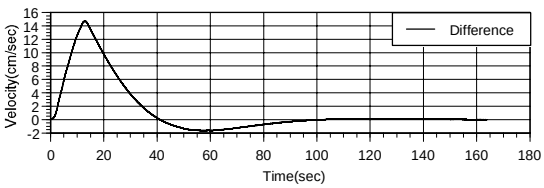

(b) Correction curve

Figure 17: Case of laboratory test (No.3)

Combined Motion of the Observed Velocity Record and the Lateral Displacement

In this study, the input ground motion is the combined motion of the base-line corrected record observed during the 1995 Kobe Earthquake at Fukushima site and the motion of lateral displacement. The input (real) – output (simulated) velocity and displacement records are shown in Figure 18(a), (b), respectively. From these figures, it is found that the uncorrected output cannot simulate the input motion. In the same way as before, the correction curve shown in Figure 18(c) is added to the output velocity record, to be able to simulate the input motion. The relationship between the correction curve and the output displacement is shown in Figure 18(d).

EXAMPLES OF CORRECTION ON THE IDEALIZED NUMERICAL ANALYSIS

The correction method of the record observed by servo velocity seismometer is shown concretely in this paragraph. From the results of movement with a constant velocity, it is shown that the coefficient curve consists of two curves. One is a curve which is during the lateral displacement and the other is after the lateral displacement. Equations of these curves are expressed as follows:

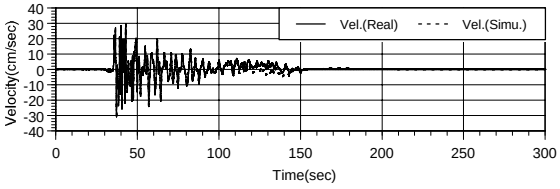

(a) Input and output velocity record

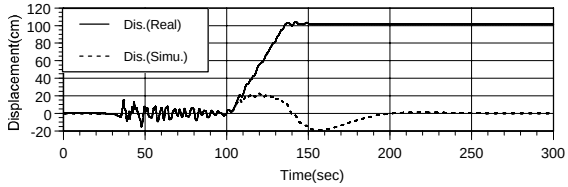

(b) Input and output displacement record

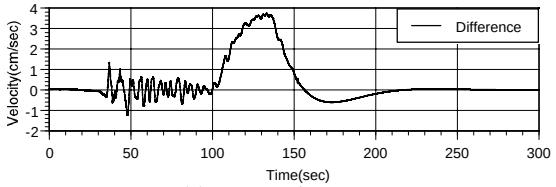

(c) Correction curve

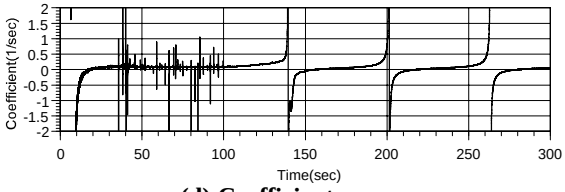

(d) Coefficient curve

Figure 18: Case of combined motion

$$f(t)=\frac{-16.48}{(t-A)}-9*10^{-5}*(t-A)^2-7*10^{-5}*(t-A)-0.188 \tag{2}$$

$$f(t)=\frac{1}{20}\tan\left(\frac{\pi}{62}(t-\tau-31.0)\right)+0.044393 \tag{3}$$

in which , A is the constant obtained by substituting the coordinates value of the intersection point between Eq. (2) and Eq. (3), τ is the time when the displacement record, which can be obtained by integration of the observed velocity record, firstly crosses zero, however this time is after the occurrence of the lateral spreading.

The coefficient curve is calculated by applying these two curves, and the processes are followings:

1) The coefficient curve after the lateral spreading is obtained by substituting the first zero crossing time for τ in Eq. (3).

2) End time of lateral spreading t_L is read from the observed velocity record and the displacement record, and $f(t_L)$ is calculated from Eq. (3) which is given process 1).

3) A is obtained by substituting t_L and $f(t_L)$ from process 2) for Eq. (2), and the coefficient curve during lateral spreading is decided.

4) The correction curve is calculated by multiplying the coefficient curve decided in process 3) and added to the observed velocity record. The correction is completed.

Here are the examples for the movement with a constant velocity and the combined motion of the observed velocity record and the lateral spreading.

First, the case of the movement with a constant velocity is explained. The coefficient curve calculated by the above-mentioned process is shown in Figure 19(a). In this figure, “calculated from observed record” means the curve shown in Figure 14(d). This figure shows that the coefficient curve is obtained properly by the above-mentioned method. Further, the correction curve is calculated from the coefficient curve and the corrected velocity record is obtained as shown in Figure 19(b) and displacement record which is integration of velocity is shown in Figure 19(c). In these figures, the real motion is shown together. From these figures, it is considered that the correction is adequately conducted and the permanent displacement can be obtained.

Next, the case of the combined motion is explained. Since it is difficult to estimate the component of the lateral spreading from the observed velocity and displacement record shown in Figure 18(a) and (b), first the low pass filtered wave is calculated. The filtered wave is shown in Figure 20(a) and (b). From these figure, it is shown that the lateral spreading starts at around 100 sec and ends at around 140sec. The first zero cross time during lateral spreading can be decided by reference to Figure 20(b) and the latter part of the coefficient curve is obtained. Further, the end time of lateral spreading is gotten and the functional value at the time is calculated. By substituting this time and functional value for Eq. (2), the former part of the coefficient curve is determined. The coefficient curve is shown in Figure 20(c) and the corrected velocity and displacement records are shown in Figure 20(d) and (e), respectively. From these figures, there is much difference between the corrected wave and real motion. Since the component of lateral spreading is extracted by low pass filter, it is not considered that the end time of lateral spreading is strict. So, the error occurred in the former part of the coefficient curve, with the result that there is a difference during the correction.

Now, we can consider the end time of the lateral spreading . Since the end time is vague due to the low pass filter, the same process is executed and the change of the end time is determined. The result is shown in Figure 21. Compared with the dotted line in Figure 14(a), it is shown that the end time is delayed 2.95 sec. The similar verification for some studied cases and on average show that the end time is delayed about 2.94 sec. By taking into account this delay, the above-mentioned process is executed again. The coefficient curve is shown in Figure 22(a). Compared with Figure 20(c), it shows similar result to the real curve. Further, the corrected velocity and displacement records are shown in Figure 22(b) and (c), respectively. By comparison with Figure 20(d) and (e), it is considered that this results become so close to the real motion.

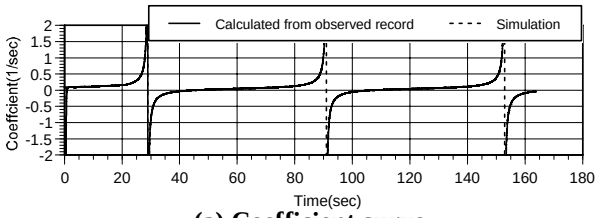

(a) Coefficient curve

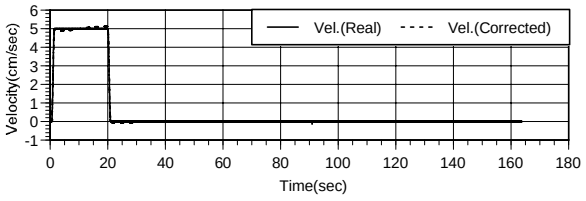

(b) Real and corrected velocity record

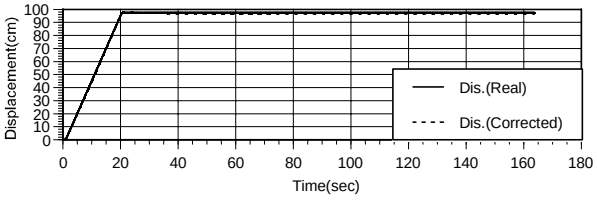

(c) Real and corrected displacement record

Figure 19: Correction result (constant velocity)

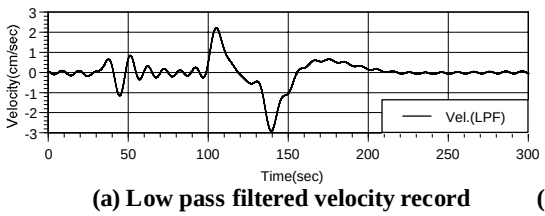

(a) Low pass filtered velocity record

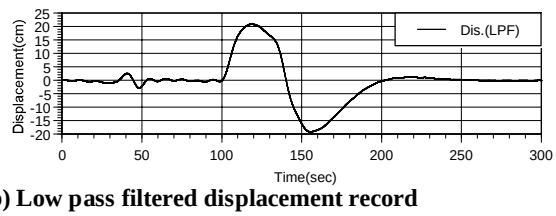

(b) Low pass filtered displacement record

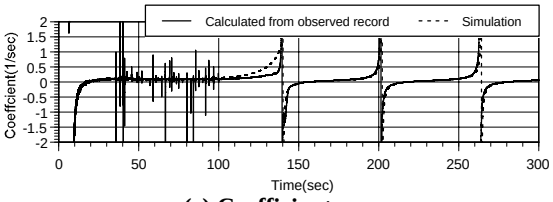

(c) Coefficient curve

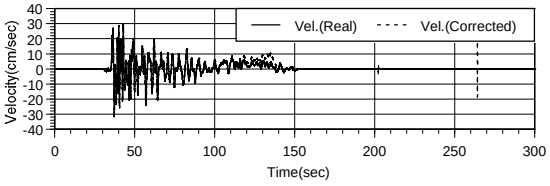

(d) Real and corrected velocity record

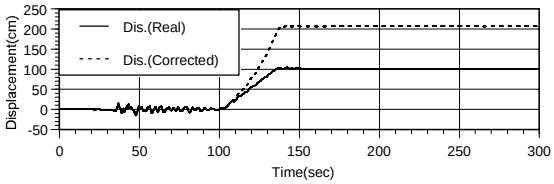

(e) Real and corrected displacement record

Figure 20: Correction result (combined motion)

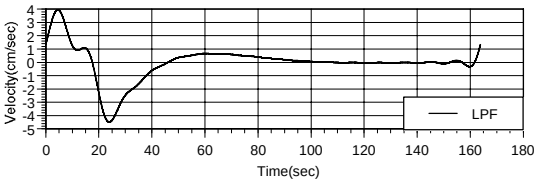

Figure 21: Low pass filtered velocity record (constant velocity)

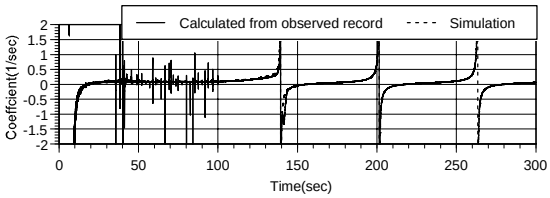

(a) Coefficient curve

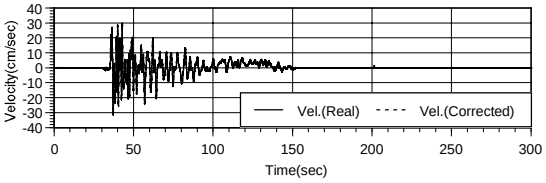

(b) Real and corrected velocity record

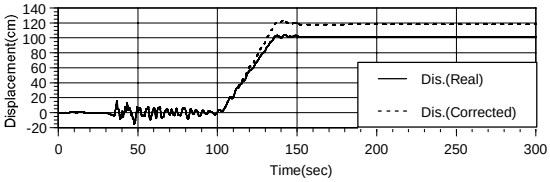

(c) Real and corrected displacement record

Figure 22: New correction result (combined motion)

CONCLUSIONS

In this study, the applicability of the method of monitoring for the permanent ground displacements using a servo velocity seismometer is investigated. The results are followings:

1) The numerical analysis of the servo velocity seismometer is able to simulate the laboratory test by accounting the change of offset value.

2) The observed record during lateral displacement is different from the real motion because of the seismometer characteristics. However, by taking into account a correction curve which is proposed in this study and adding the correction to the output velocity record, the ground displacement can be closely matched to the actual motion of the servo velocity seismometer.

REFERENCES

Kagawa, T., Irikura, K. and Yokoi, I.(1996), "Restoring clipped records of near-field strong ground motion during the 1995 Hyogo-ken Nanbu (Kobe), Japan Earthquake", *Journal of Natural Disaster Science*, Vol.18, pp.43-57

Toki, K., Sawada, S., Morikawa, H. and Inukai, N.(1997), "Measurement of the permanent ground displacement using a servo velocity seismometer", *JSCE Kansai Chapter/Proc. of Annual Conference of Civil Engineers '97*, I-36-1 & 2

Yokoi, I.(1992), "Servo velocity seismometer", *Sensor Technique*, pp.69-72